Three-Dimensional Topological Insulators on the Pyrochlore Lattice

H.-M. Guo and M. Franz

Department of Physics and Astronomy, University of British Columbia, Vancouver, BC, Canada V6T 1Z1

(Received 5 August 2009; published 13 November 2009)

Electrons hopping on the sites of a three-dimensional pyrochlore lattice are shown to form topologically nontrivial insulating phases when the spin-orbit (SO) coupling and lattice distortions are present. Of 16 possible topological classes 9 are realized for various parameters in this model. Specifically, at half-filling an undistorted pyrochlore lattice with a SO term yields a "pristine" strong topological insulator with a Z_2 index (1;000). At quarter filling various strong and weak topological phases are obtained provided that both SO coupling and uniaxial lattice distortion are present. Our analysis suggests that many of the nonmagnetic insulating pyrochlores could be topological insulators.

DOI: 10.1103/PhysRevLett.103.206805 PACS numbers: 73.43.−f, 72.25.Hg, 73.20.−r, 85.75.−d

According to recent pioneering theoretical studies [1,2] all time-reversal ($\mathcal{T}$) invariant (nonmagnetic) band insulators in three spatial dimensions can be classified into 16 topological classes distinguished by a four-component topological index (ν_0; $\nu_1\nu_2\nu_3$) with $\nu_\alpha = 0, 1$. Ordinary "trivial" band insulators have an index (0;000) and, in general, possess no robust surface states. When some of the ν differ from zero then the insulator is said to be topologically nontrivial and, as a result, possesses topologically protected surface states on at least some of its surfaces. When $\nu_0 = 1$ surface states exist on *all* surfaces and are in addition robust with respect to weak nonmagnetic disorder. This is referred to as a strong topological insulator (STI). Strong topological insulators are predicted to exhibit a host of unusual phenomena associated with their nontrivial surface states. These include proximity-induced exotic superconducting state with Majorana fermions bound to a vortex [3], spin-charge separated solitonic excitations [4,5], and, in a thin film geometry, an unconventional excitonic state with fractionally charged vortices [6]. There are also interesting bulk manifestations of STI physics such as the "axion" electromagnetic response [7,8] and the topologically protected fermion modes localized along the core of a crystal dislocation [9].

Topologically nontrivial insulating phases have been predicted to occur [10–12] and subsequently experimentally discovered [13–15] in several two- and three-dimensional crystalline solids. Vigorous search for new materials in this class is ongoing. With the goal of enlarging the space of candidate crystalline structures that can potentially support topologically nontrivial insulating phases we study in this Letter a class of tight-binding models with SO coupling for electrons moving on the *pyrochlore* lattice displayed in Fig. 1(a). Our model belongs to the class of 3D "frustrated hopping" models [16] and the motivation for this study comes in part from our recent finding that electrons on the kagome lattice, a canonical example of the frustrated structure in two dimensions, form a 2D topological insulator when SO coupling is present [17].

Our main finding here is that, quite generically, whenever electrons hopping on the pyrochlore lattice acquire a band gap from SO interactions the resulting state is either a STI or a weak topological insulator (WTI), defined as a state with $\nu_0 = 0$ but at least one $\nu_{i=1,2,3} \neq 0$. At quarter filling the physics leading to the TI behavior on the pyrochlore lattice is somewhat similar to the Fu-Kane-Mele (FKM) model on the diamond lattice [1]. SO interaction produces Dirac-type spectrum at the three **X** points of the Brillouin zone (BZ), Fig. 1(b), and uniaxial crystal distortion is needed to open up a gap. The resulting Z_2 indices are however different from FKM. At half filling, the band

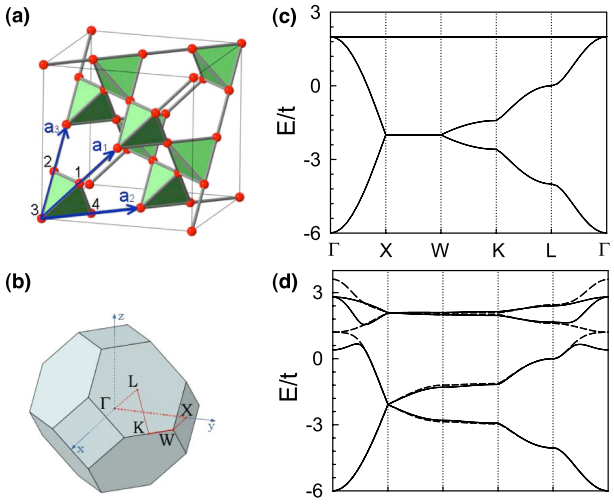

FIG. 1 (color online). (a) Pyrochlore lattice is a face-centered cubic Bravais lattice with a 4-point basis forming a shaded tetrahedron. (b) The first Brillouin zone of the fcc lattice with high-symmetry lines and points indicated. (c) Band structure of the tight-binding model Eq. (1). (d) Band structure with spin-orbit coupling Eq. (3) for $\lambda = -0.1t$ (solid line) and $\lambda = 0.1t$ (dashed line).

crossing occurs at the $\mathbf{\Gamma}$ point and is *quadratic* rather than Dirac-like. In this case SO coupling by itself opens up a gap and no lattice distortion is required. This is, to our knowledge, a unique behavior, which produces a highly symmetric "pristine" STI characterized by index (1;000).

We now supply the technical details supporting these claims. Our starting point is the tight-binding model

$$H_0 = -t \sum_{\langle ij \rangle \sigma} c^\dagger_{i\sigma} c_{j\sigma}, \tag{1}$$

where $c^\dagger_{i\sigma}$ creates an electron with spin σ on the site $\mathbf{r}_i$ of the pyrochlore lattice and $\langle ij \rangle$ denotes nearest neighbors. In momentum space Eq. (1) becomes $H_0 = \sum_{\mathbf{k}\sigma} \Psi^\dagger_{\mathbf{k}\sigma} \mathcal{H}^0_{\mathbf{k}} \Psi_{\mathbf{k}\sigma}$ with $\Psi_{\mathbf{k}\sigma} = (c_{1\mathbf{k}\sigma}, c_{2\mathbf{k}\sigma}, c_{3\mathbf{k}\sigma}, c_{4\mathbf{k}\sigma})^T$ and $\mathcal{H}^0_{\mathbf{k}}$ of the form

$$-2t \begin{pmatrix} 0 & \cos(k_x - k_y) & \cos(k_x + k_z) & \cos(k_y - k_z) \\ & 0 & \cos(k_y + k_z) & \cos(k_x - k_z) \\ & & 0 & \cos(k_x + k_y) \\ & & & 0 \end{pmatrix}.$$

The lower triangle of the matrix is understood to be filled so that the matrix is Hermitian. The spectrum of $\mathcal{H}^0_{\mathbf{k}}$, Fig. 1(c), consists of two degenerate flat bands $E^{(3,4)}_{\mathbf{k}} = 2t$ and two dispersive bands

$$E^{(1,2)}_{\mathbf{k}} = -2t[1 \pm \sqrt{1 + A_{\mathbf{k}}}], \tag{2}$$

with $A_{\mathbf{k}} = \cos(2k_x)\cos(2k_y) + \cos(2k_x)\cos(2k_z) + \cos(2k_y)\cos(2k_z)$. $E^{(2)}_{\mathbf{k}}$ touches the two flat bands at the $\mathbf{\Gamma}$ point and the band crossing is quadratic. $E^{(1)}_{\mathbf{k}}$ and $E^{(2)}_{\mathbf{k}}$ touch along the lines located at the diagonals of the square faces of the BZ.

At the half-filling, bands 1 and 2 are filled completely, and the two degenerate flat bands are empty. This state is a gapless band insulator. We now seek terms bilinear in the electron operators that lead to the formation of a gap at the quadratic band crossing point. We focus on perturbations that do not further break the translational symmetry of H_0 and preserve $\mathcal{T}$. A natural term to consider is a SO interaction of the form

$$H_{\mathrm{SO}} = i\lambda \sum_{\langle\langle ij \rangle\rangle \alpha\beta} (\mathbf{d}^1_{ij} \times \mathbf{d}^2_{ij}) \cdot \boldsymbol{\sigma}_{\alpha\beta} c^\dagger_{i\alpha} c_{j\beta}, \tag{3}$$

where λ is the SO coupling strength, $\mathbf{d}^{1,2}_{ij}$ are nearest-neighbor vectors traversed between second neighbors i and j, and $\boldsymbol{\sigma}$ is the vector of Pauli spin matrices. Since $\mathbf{d}^{1,2}_{ij}$ lie in three-dimensional space, the Hamiltonian does not decouple for the two spin projections and in k space becomes an 8×8 matrix. Figure 1(d) shows the spectrum of $\mathcal{H}^0_{\mathbf{k}} + \mathcal{H}^{\mathrm{SO}}_{\mathbf{k}}$. For $\lambda > 0$ it remains gapless but for $\lambda < 0$ a gap $\Delta_{\mathrm{SO}} = 24|\lambda|$ opens at the $\mathbf{\Gamma}$ point. This peculiar behavior can be understood by studying the matrix $\mathcal{H}^0_{\mathbf{k}} + \mathcal{H}^{\mathrm{SO}}_{\mathbf{k}}$ at $\mathbf{k} = 0$. It is easy to see that the SO coupling splits the sixfold degeneracy into a twofold degenerate level at $2t + 16\lambda$ and a four-fold degenerate level at $2t - 8\lambda$. For $\lambda/t < 0$ this allows the four-fold degenerate flat band to split off from the twofold degenerate dispersive band. We shall see momentarily that the resulting state is a STI.

Although the SO interaction reduces the degeneracies of bands 1 and 2, they still touch at three inequivalent Dirac points $\mathbf{X}_r = 2\pi\hat{r}/a$, where $r = x, y, z$. At quarter-filling band 1 is fully occupied and it is interesting to ask what $\mathcal{T}$-invariant perturbation would open up a gap at the Dirac points. We have been able to identify two such terms: (i) lattice distortions leading to anisotropy in the nearest-neighbor hopping amplitudes, and (ii) modulations in on-site potentials within the unit cell. Both of these preserve the unit cell, the inversion symmetry and $\mathcal{T}$.

For the lattice distortions, since there are six hopping amplitudes in the unit cell Fig. 1(a), one has many choices. We now describe four "basic" highly symmetric anisotropy patterns that open up gaps with equal magnitude at all three Dirac points. We then classify the resulting insulating phases and argue that this classification is in fact exhaustive. The basic distortion, labeled by $l = 1, 2, 3, 4$, is obtained by selecting site l in the unit cell and changing

$$t \rightarrow t \pm \eta. \tag{4}$$

The $+$ sign refers to the six bonds emanating from site l whereas the $-$ sign refers to all remaining bonds. This can be achieved by deforming the crystal along the axis passing through the site l and the center of the tetrahedron. For pattern 1, the Hamiltonian $\mathcal{H}^{\mathrm{dis}}_{\mathbf{k}}$ describing this modulation takes the form

$$-2\eta \begin{pmatrix} 0 & \cos(k_x - k_y) & \cos(k_x + k_z) & \cos(k_y - k_z) \\ & 0 & -\cos(k_y + k_z) & -\cos(k_x - k_z) \\ & & 0 & -\cos(k_x + k_z) \\ & & & 0 \end{pmatrix}$$

for both spin projections. For $l = 2, 3, 4$ the signs in front of the cosine terms are permuted in an obvious way. The full expression for the spectrum of $\mathcal{H}^0_{\mathbf{k}} + \mathcal{H}^{\mathrm{SO}}_{\mathbf{k}} + \mathcal{H}^{\mathrm{dis}}_{\mathbf{k}}$ is complicated but it is easy to establish that gaps $\Delta_{\mathrm{dis}} = 4|\eta|$ simultaneously open up at all the Dirac points.

As mentioned above a gap also opens up as a result of on-site potential modulation. A convenient symmetric choice defines pattern l as $\epsilon_l = 3\mu$ and $\epsilon_{k\neq l} = -\mu$ with μ a constant.

We now study the topological classes of these insulating phases. As shown in Ref. [11] the Z_2 topological invariants $(\nu_0; \nu_1\nu_2\nu_3)$ are easy to evaluate when a crystal possesses inversion symmetry. The invariants can be determined from knowledge of the parity eigenvalues $\xi_{2m}(\mathbf{\Gamma}_i)$ of the $2m$th occupied energy band at the 8 $\mathcal{T}$-invariant momenta (TRIM) $\mathbf{\Gamma}_i$ that satisfy $\mathbf{\Gamma}_i = \mathbf{\Gamma}_i + \mathbf{G}$. The 8 TRIM in our system can be expressed in terms of primitive reciprocal lattice vectors as $\mathbf{\Gamma}_{i=(n_1n_2n_3)} = (n_1\mathbf{b}_1 + n_2\mathbf{b}_2 + n_3\mathbf{b}_3)/2$, with $n_j = 0, 1$. Then ν_α is determined by the product

$(-1)^{\nu_0} = \prod_{n_j=0,1} \delta_{n_1 n_2 n_3}$, and $(-1)^{\nu_{i=1,2,3}} = \prod_{n_{j\neq i}=0,1; n_i=1} \delta_{n_1 n_2 n_3}$, where $\delta_i = \prod_{m=1}^{N} \xi_{2m}(\mathbf{\Gamma}_i)$.

Our model is inversion symmetric for all perturbations discussed above and so we can use this method to find ν. If we select site 3 of the unit cell, Fig. 1(a), as the center of inversion then the parity operator acts as $\mathcal{P}[\psi_1(\mathbf{r}), \psi_2(\mathbf{r}), \psi_3(\mathbf{r}), \psi_4(\mathbf{r})] = [\psi_1(-\mathbf{r} - \mathbf{a}_1), \psi_2(-\mathbf{r} - \mathbf{a}_3), \psi_3(-\mathbf{r}), \psi_4(-\mathbf{r} - \mathbf{a}_2)]$ on the four-component electron wave function in the unit cell labeled by vector $\mathbf{r}$. In momentum space and including spin the parity operator becomes a diagonal 8×8 matrix $\mathcal{P}_{\mathbf{k}} = \mathrm{diag}(e^{-i\mathbf{a}_1\cdot\mathbf{k}}, e^{-i\mathbf{a}_3\cdot\mathbf{k}}, 1, e^{-i\mathbf{a}_2\cdot\mathbf{k}}) \otimes \mathrm{diag}(1, 1)$. It is straightforward to obtain the eigenstates of $\mathcal{H}_{\mathbf{\Gamma}_i}$ and the parity eigenvalues of the occupied bands numerically, then determine the Z_2 invariants. At half filling, we find that $\delta = 1$ at the $\mathbf{\Gamma}$ point and $\delta = -1$ at other TRIM, so the spin-orbit phase is a (1;000) strong topological insulator.

At quarter filling, we find 8 Z_2 classes, depending on the type of the distortion. Four of these are STIs and 4 are WTIs (Table I). The distinction between STI and WTI is easy to understand on physical grounds by considering some limiting cases. In the limit $\eta \to -t$ the electrons can only move in decoupled parallel planes, each forming a 2D kagome lattice. Electrons hopping in the kagome lattice with spin-orbit interaction of the form (3) produce a 2D topological insulator [17]. A collection of such planes results in WTI even after interplane coupling is restored. When $\eta \to t$, on the other hand, the resulting structure remains 3-dimensional and STI behavior prevails.

To develop better understanding for the insulating phases at quarter filling we now examine the form of the low-energy Hamiltonians governing the excitations in the vicinity of the three Dirac points. This is obtained by linearizing $\mathcal{H}^0_{\mathbf{k}} + \mathcal{H}^{\mathrm{SO}}_{\mathbf{k}} + \mathcal{H}^{\mathrm{dis}}_{\mathbf{k}}$ near $\mathbf{X}_r$ and subsequently projecting onto the subspace associated with bands 1 and 2. Near the $\mathbf{X}_z$ point we rescale momenta as $12\lambda k_x(k_y) \to k_x(k_y)$ and $4t k_z \to k_z$, and obtain a three-dimensional Dirac Hamiltonian,

$$\mathcal{H}^{z}_{\mathrm{eff}} = \tau^x k_z + (\sigma^x k_x + \sigma^y k_y)\tau^y + 2m^l_z \tau^z. \qquad (5)$$

$\mathcal{H}^{x,y}_{\mathrm{eff}}$ are the same with x, y and z permuted in k_i and σ^i. Index l in the mass labels the distortion pattern and the values of masses are shown in Table I. We observe that $l =$ 1, 2, 3, 4 and two possible signs of η exhaust all possible sign combinations for the three Dirac masses. Since the Z_2 index can only change when at least one of the masses goes through zero it follows that our classification in Table I is exhaustive. In particular given *any* cell-periodic pattern of bond distortions and on-site energies the Z_2 class is uniquely determined by the pattern of the Dirac mass signs listed in Table I.

TABLE I. Z_2 class for the insulators at quarter filling and the corresponding Dirac mass values in the low-energy effective Hamiltonian (5) for different distortion patterns and arbitrary $\lambda \neq 0$.

Dis	Mass (m_x, m_y, m_z)		Z_2 class		Z_2 class
1	$-\eta, \eta, \eta$	$\eta < 0$	0;100	$\eta > 0$	1;100
2	$\eta, -\eta, \eta$	$\eta < 0$	0;001	$\eta > 0$	1;001
3	$\eta, \eta, -\eta$	$\eta < 0$	0;111	$\eta > 0$	1;111
4	$-\eta, -\eta, -\eta$	$\eta < 0$	0;010	$\eta > 0$	1;010

One can also study the origin of the topologically protected surface states using the above low-energy Hamiltonian (5). Consider, for the sake of concreteness, a boundary between two different phases, running along, say, the $z = 0$ plane in real space. We take distortion pattern 2, $\eta < 0$ in the left half-space and pattern 1, $\eta > 0$ in the right half-space. The mass m_z necessarily undergoes a sign change across the $z = 0$ boundary. Such a soliton mass profile is known to produce massless states in the associated Dirac equation, localized near the boundary [18]. Specifically, 3D Dirac equation

$$[-i\tau^x \partial_z + (\sigma^x k_x + \sigma^y k_y)\tau^y + m(z)\tau^z]\phi_{\mathbf{k}}(z) = E\phi_{\mathbf{k}}(z) \qquad (6)$$

with $m(z \to \pm\infty) = \pm m_0$ has gapless solutions

$$\phi_{\pm\mathbf{k}}(z) = \frac{1}{\sqrt{2}} \begin{pmatrix} \pm\varphi_{\mathbf{k}} \\ \pm i\varphi_{\mathbf{k}} \\ 1 \\ i \end{pmatrix} e^{-\int_0^z m(z')dz'}, \qquad (7)$$

extended in the $z = 0$ plane but localized in the transverse direction, with linearly dispersing energy $E_{\pm} = \pm k$, where $\varphi_{\mathbf{k}} = (k_x - ik_y)/k$ and $k = \sqrt{k_x^2 + k_y^2}$. The number of gapless states determines the topological class of the phases on two sides of the boundary. If the number is odd, the boundary is between a WTI and a STI phase. If the number is even, the boundary is between two WTI or two STI phases.

To further support our identification of topological classes given above, we have performed numerical diagonalizations of the lattice Hamiltonian $H_0 + H_{\mathrm{SO}} + H_{\mathrm{dis}}$ using the slab geometry. Figure 2 shows the two-dimensional band structures of a representative sample of the insulating phases obtained for various patterns of crystal distortions. We consider a slab geometry with two 111 surfaces, and plot band energies along lines that connect the four surface TRIM. Four bulk bands are clearly visible and there are also surface states some of which traverse the gap.

At half filling the system is in the (1;000) STI phase (we take $\lambda < 0$). Irrespective of the lattice distortion there is a single Fermi surface (FS) around the $\mathbf{\Gamma}$ point for each surface. Since the two surfaces are inequivalent in this geometry the Fermi surfaces are also different.

At quarter filling more possibilities arise. In the WTI phases (0;111) and (0;100) the (even) number of surface FS

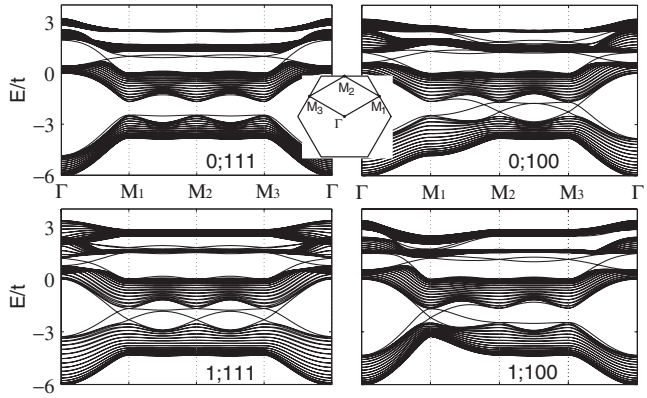

FIG. 2. Band structures for a slab with a 111 face in various insulating phases with $\lambda = -0.1t$ and $|\eta| = 0.2t$. The Z_2 index refers to quarter filling. At half filling all four panels represent a (1;000) STI. The inset shows the surface BZ with high-symmetry points marked.

depends on the orientation of the surface vector with respect to $(\nu_1\nu_2\nu_3)$, as discussed in Ref. [1]. For instance the 111 surface has no surface FS in the (0;111) insulator while there are two per surface in the (0;100) phase. In the STI phase (1;100) and (1;111) there are 1 and 3 Dirac points on TRIM, respectively. Near each such Dirac point a pair of robust spin-filtered states exists. Crossings at other momenta can occur; however there is always an even number of such crossings, confirming the above arguments.

Many insulating compounds with pyrochlore structure are known to exist [19]. These follow a formula $A_2B_2O_7$ with A typically a rare earth and B a transition metal element. Existing experimental studies so far focused mostly on the magnetic pyrochlores due to their promise as candidate systems for exotic spin liquid and spin ice ground states brought about by the geometric frustration inherent to the pyrochlore structure. Our theoretical results show that *nonmagnetic* pyrochlores with strong SO coupling could exhibit interesting physics. One promising candidate is pyrochlore $Cd_2Os_2O_7$ which shows insulating behavior below 225 K [20]. Band structure calculations in this compound favor nonmagnetic ground state and indicate strong SO effects [21]. Also promising are the Ir-based pyrochlores $A_2Ir_2O_7$ since various Ir-based transition metal oxides have been predicted and reported to exhibit significant SO effects [22–24]. In addition, for $A =$ Nd, Sm, Eu metal-insulator transitions have been reported at 36, 117 and 120 K, respectively [25].

Whether a particular pyrochlore is a topological insulator can be established only through a detailed band structure calculation or an experimental measurement. These are clearly beyond the scope of our present study. It is however very encouraging to note that, in a preprint that appeared after the completion of this work, Pesin and Balents [26] derived a semirealistic tight-binding model for $A_2Ir_2O_7$ ($A =$ Pr, Eu) and found band structures for active orbitals closely resembling that displayed in Fig. 1(d) for $\lambda/t < 0$. They find, in agreement with our results, that the system at half filling is a pristine strong topological insulator. We conclude that pyrochlore oxides are likely to open a new frontier in the quest for technologically useful topological insulators and, more generally, exciting new topological states of quantum matter. Clearly, detailed band structure calculations and careful experimental studies of these families of materials are warranted.

Authors are indebted to J. Moore, G. Rosenberg, B. Seradjeh and C. Weeks for stimulating discussions. Support for this work came from NSERC, CIfAR and The China Scholarship Council.

[1] L. Fu, C. L. Kane, and E. J. Mele, Phys. Rev. Lett. **98**, 106803 (2007).
[2] J. E. Moore and L. Balents, Phys. Rev. B **75**, 121306(R) (2007).
[3] L. Fu and C. L. Kane, Phys. Rev. Lett. **100**, 096407 (2008).
[4] Y. Ran, A. Vishwanath, and D.-H. Lee, Phys. Rev. Lett. **101**, 086801 (2008).
[5] X.-L. Qi and S.-C. Zhang, Phys. Rev. Lett. **101**, 086802 (2008).
[6] B. Seradjeh, J. E. Moore, and M. Franz, Phys. Rev. Lett. **103**, 066402 (2009).
[7] X.-L. Qi, T. L. Hughes, and S.-C. Zhang, Phys. Rev. B **78**, 195424 (2008).
[8] A. M. Essin, J. E. Moore, and D. Vanderbilt, Phys. Rev. Lett. **102**, 146805 (2009).
[9] Y. Ran, Y. Zhang, and A. Vishwanath, Nature Phys. **5**, 298 (2009).
[10] B. A. Bernevig, T. L. Hughes, and S.-C. Zhang, Science **314**, 1757 (2006).
[11] L. Fu and C. L. Kane, Phys. Rev. B **76**, 045302 (2007).
[12] H. Zhang, C.-X. Liu, X.-L. Qi, X. Dai, Z. Fang, and S.-C. Zhang, Nature Phys. **5**, 438 (2009).
[13] M. König *et al.*, Science **318**, 766 (2007).
[14] D. Hsieh *et al.*, Nature (London) **452**, 970 (2008).
[15] Y. Xia *et al.*, Nature Phys. **5**, 398 (2009).
[16] D. L. Bergman, C. Wu, and L. Balents, Phys. Rev. B **78**, 125104 (2008).
[17] H.-M. Guo and M. Franz, Phys. Rev. B **80**, 113102 (2009).
[18] R. Jackiw and C. Rebbi, Phys. Rev. D **13**, 3398 (1976).
[19] M. A. Subramanian, G. Aravamudan, and G. V. S. Rao, Prog. Solid State Chem. **15**, 55 (1983).
[20] D. Mandrus *et al.*, Phys. Rev. B **63**, 195104 (2001).
[21] D. J. Singh, P. Blaha, K. Schwarz, and J. O. Sofo, Phys. Rev. B **65**, 155109 (2002).
[22] G. Chen and L. Balents, Phys. Rev. B **78**, 094403 (2008).
[23] A. Shitade *et al.*, Phys. Rev. Lett. **102**, 256403 (2009).
[24] B. J. Kim *et al.*, Science **323**, 1329 (2009).
[25] K. Matsuhira *et al.*, J. Phys. Soc. Jpn. **76**, 043706 (2007).
[26] D. A. Pesin and L. Balents, arXiv:0907.2962.